PASJ: Publ. Astron. Soc. Japan **61**, L7–L11, 2009 June 25

Global Radiation-Magnetohydrodynamic Simulations of Black-Hole Accretion Flow and Outflow: Unified Model of Three States

Ken OHSUGA,[1,2] Shin MINESHIGE,[3] Masao MORI,[4] and Yoshiaki KATO[5]
[1]*National Astronomical Observatory of Japan, 2-1-1 Osawa, Mitaka, Tokyo 181-8588*
[2]*Institute of Physical and Chemical Research (RIKEN), 2-1 Hirosawa, Wako, Saitama 351-0198*
[3]*Department of Astronomy, Graduate School of Science, Kyoto University, Kyoto 606-8502*
[4]*Center for Computational Sciences, University of Tsukuba, Tsukuba, Ibaraki 305-8577*
[5]*JAXA / Institute of Space and Astronautical Science, 3-1-1 Yoshinodai, Sagamihara, Kanagawa 229-8510*

(Received 2008 October 2; accepted 2009 March 16)

Abstract

Black-hole accretion systems are known to possess several distinct modes (or spectral states), such as low/hard state and high/soft state. Since the dynamics of the corresponding flows is distinct, theoretical models were separately considered for each state. We here propose a unified model based on our new, global, two-dimensional radiation-magnetohydrodynamic simulations. By controlling a density normalization we could for the first time reproduce three distinct modes of accretion flow and outflow with one numerical code. When the density is large (model A), a geometrically thick, very luminous disk forms, in which photon trapping takes place. When the density is moderate (model B), the accreting gas can effectively be cooled by emitting radiation, thus generating a thin disk, i.e., a soft-state disk. When the density is too low for radiative cooling to be important (model C), a disk becomes hot, thick, and faint; i.e., a hard-state disk. The magnetic energy is amplified within the disk up to about twice, 30%, and 20% of the gas energy in models A, B, and C, respectively. Notably, the disk outflows with helical magnetic fields, which are driven either by radiation-pressure force or magnetic-pressure force, are ubiquitous in any accretion modes. Finally, our simulations are consistent with the phenomenological α-viscosity prescription; that is, the disk viscosity is proportional to the pressure.

Key words: accretion, accretion disks — black hole physics — ISM: jets and outflows — magnetohydrodynamics: MHD — radiative transfer

1. Introduction

Extensive studies of disk accretion flows started in the 1960's. The standard disk model, and then the slim disk model and the radiatively inefficient accretion flow (RIAF) model were proposed for explaining a variety of accretion modes (Shakura & Sunyaev 1973; Ichimaru 1977; Rees et al. 1982; Abramowicz et al. 1988; Narayan & Yi 1994). These models are successful, but have some limitations. For example, the disk viscosity, the most important key ingredient for accretion-disk theory, is prescribed by a phenomenological α-viscosity model, whereby the viscous torque is proportional to the pressure (Kato et al. 2008), although its physical basis is not clear. Since they are (radially) one-dimensional models, they cannot describe multi-dimensional motion, such as outflow and internal circulation. Complex coupling between radiation, magnetic fields, and matter has not been accurately solved, either.

Since the disk viscosity is likely to be of magnetic origin (Balbus & Hawley 1991), multi-dimensional global magnetohydrodynamics (MHD) simulations are being rather extensively performed recently as a model for disks with low luminosities (Matsumoto 1999; Machida et al. 2000; Hawley & Krolik 2001; Koide et al. 2001; De Villiers et al. 2003; Hawley & Krolik 2006; Fragile & Meier 2009). Such non-radiative MHD simulations, however, cannot explain higher luminosity states, since strong matter-radiation coupling is expected. As an independent approach, several groups performed two-dimensional radiation-hydrodynamic (RHD) simulations of very luminous flow since the 1980's (Eggum et al. 1988; Okuda & Fujita 2000; Ohsuga et al. 2005; Ohsuga 2006). Those simulations were, however, of the non-MHD type, and so they were obliged to rely on a phenomenological α-viscosity model. Therefore, multi-dimensional radiation-MHD (RMHD) simulations are unavoidable. Such simulations were attempted in the past (e.g., Turner et al. 2003; Hirose et al. 2006), but are restricted to local simulations performed under shearing-box approximations, and hence global coupling of magnetic fields was artificially quenched there.

Here, we report for the first time on the results of global two-dimensional RMHD simulations with a motivation to establish a unified view of the accretion flow and outflow around the black-holes.

2. Numerical Method

Our method of calculations is an extension of that of MHD simulations (e.g., Kato et al. 2004). We use cylindrical

coordinates (r, φ, z), where r is the radial distance, φ is the azimuthal angle, and z is the vertical distance. We assume that the flow is non-self-gravitating, reflection symmetric relative to equatorial plane, and axisymmetric with respect to the rotation axis. General relativistic effects are incorporated by the pseudo-Newtonian potential (Paczynsky & Wiita 1980). For opacity, we consider Thomson scattering, free-free absorption, and bound-free absorption (Rybicki & Lightman 1979; Hayashi et al. 1962). The energy equations of gas and radiation are given by

$$\frac{\partial E_{\rm gas}}{\partial t} + \nabla\cdot(E_{\rm gas}\boldsymbol{v}) = -p_{\rm gas}\nabla\cdot\boldsymbol{v} - 4\pi\kappa B + c\kappa E_{\rm rad} + \frac{4\pi}{c^2}\eta J^2 \quad (1)$$

and

$$\frac{\partial E_{\rm rad}}{\partial t} + \nabla\cdot(E_{\rm rad}\boldsymbol{v}) = -\nabla\cdot\boldsymbol{F}_{\rm rad} - \nabla\boldsymbol{v} : \boldsymbol{P}_{\rm rad} + 4\pi\kappa B - c\kappa E_{\rm rad}, \quad (2)$$

where $E_{\rm gas}$ is the internal energy density of the gas, $\boldsymbol{v}$ the velocity, $p_{\rm gas}$ the gas pressure ($\equiv 2E_{\rm gas}/3$), B the blackbody intensity, J the electric current, $E_{\rm rad}$ the radiation energy density, $\boldsymbol{F}_{\rm rad}$ the radiative flux, $\boldsymbol{P}_{\rm rad}$ the radiation pressure tensor, and κ the absorption opacity. We adopt the anomalous resistivity, η, which is the same as that used in Kato et al. (2004):

$$\eta = \begin{cases} 0 & \text{for } v_{\rm d} < v_{\rm crit} \\ \eta_{\rm max}\left[\left(\dfrac{v_{\rm d}}{v_{\rm crit}}\right) - 1\right]^2 & \text{for } v_{\rm crit} \le v_{\rm d} < 2v_{\rm crit}, \\ \eta_{\rm max} & \text{for } v_{\rm d} \ge 2v_{\rm crit} \end{cases} \quad (3)$$

where $v_{\rm d} \equiv J/\rho$ is the electron drift velocity, $v_{\rm crit} \equiv 0.01c$ the critical velocity, and $\eta_{\rm max} \equiv 10^{-3}cR_S$ the maximum resistivity with R_S being the Schwarzschild radius. This form of anomalous resistivity was proposed by Yokoyama and Shibata (1994) to account for the occurrence of fast reconnections in solar flares. The MHD related terms were solved by the modified Lax-Wendroff scheme (Rubin & Burstein 1967). We employed the flux-limited diffusion (FLD) approximation to solve the radiation energy equation (Levermore & Pomraning 1981). The radiation energy transport via the radiative flux was solved based on an implicit method, where we separately treated radiative fluxes in the radial and vertical directions using the Thomas method for a matrix inversion. The gas-radiation interaction was also solved with the implicit method, which is basically the same as that described by Turner and Stone (2001). An advection term in the energy equation of the radiation was solved with the explicit method, in which an integral formulation was used to generate a conservative differencing scheme. We performed a test of two-dimensional radiation propagation (Turner & Stone 2001), finding that the energy loss is less than 0.005% in 600 steps, from which we estimated the error in the energy conservation not to exceed 0.08% during the photon traveling timescale in our simulations.

The grid, we used, extended from $3\,R_S$ to $103\,R_S$ in the radial direction and from 0 to $91.6\,R_S$ in the vertical direction. The grid spacing was uniform, $0.2\,R_S$, in both directions. We adopted free boundary conditions for the matter and magnetic fields; i.e., the matter could freely go out, but not to come in, and the magnetic fields could not change across the boundary. We assumed that radiation goes out with the radiation flux of $cE_{\rm rad}$, except at $r = 3\,R_S$ and $z > 3\,R_S$, through which no radiation could go out. We assumed the black-hole mass to be $10\,M_\odot$. In the future we will perform simulations in which we will put the boundary condition at around R_S and to solve both side of the midplane.

We started calculations with a rotating torus, in which the magnetic fields were purely poloidal (plasma-β = 100) and closed loops in the torus, being located at around $40\,R_S$ embedded in a non-rotating isothermal corona. Our initial conditions were the same as those of model B in Kato et al. (2004), except that the density of the corona was 0.05-times as large as that one. We evolved the initial torus by solving non-radiative MHD equations for 1 s. We then assigned the density normalization (ρ_0), the density at the center of the initial torus, and turned on the radiation terms. We calculated three models in total, by setting $\rho_0 = 1\,{\rm g\,cm^{-3}}$ (model A), $10^{-4}\,{\rm g\,cm^{-3}}$ (model B), and $10^{-8}\,{\rm g\,cm^{-3}}$ (model C). Since radiation loss rate depends on the density, we could reproduce the three distinct regimes of accretion flow.

3. Results

3.1. Accretion Flows

Figure 1 clearly shows that the flow patterns differ significantly among the three models. The typical mass-accretion rate ($\dot{M}_{\rm acc}$), luminosity (L), density (ρ) and temperature (T), as well as other important quantities, are summarized in table 1.

In model A with a relatively large density normalization, the mass-accretion rate exceeds the Eddington rate, $L_{\rm E}/c^2$, with $L_{\rm E}$ being the Eddington luminosity. The disk is optically and geometrically thick. Photons can not easily go out from the surface due to a large optical depth, so that radiative cooling is restricted. We confirmed the photon-trapping effects. The disk is supported by radiation pressure. Circular motion appears in the disk region. Since $L \gtrsim L_{\rm E}$, this model corresponds to a two-dimensional version of the slim-disk model. The calculated temperature and density are also consistent.

In model B with a moderate density normalization, a geometrically thin disk forms because of efficient radiative cooling. The disk is optically thick and supported mainly by radiation pressure, which is slightly greater than the gas pressures. Such properties, as well as the temperature and density, agree with those of the standard disk model. It might be noted well that the flow in model B does not reach a quasi-steady state, since the viscous timescale is about 45 s at $r = 10\,R_S$, whereas the elapsed time is 8 s. In a forthcoming paper we will report on finer mesh calculations with adequate grid spacing, by which we will be able to investigate the detailed, internal structure of the thin disk.

In model C with a small density normalization, the density is too low for radiative cooling to be important. The disk is filled with hot rarefied plasmas, and is geometrically thick but optically thin. We have found significant circular motion inside the disk. This model corresponds to the RIAF model.

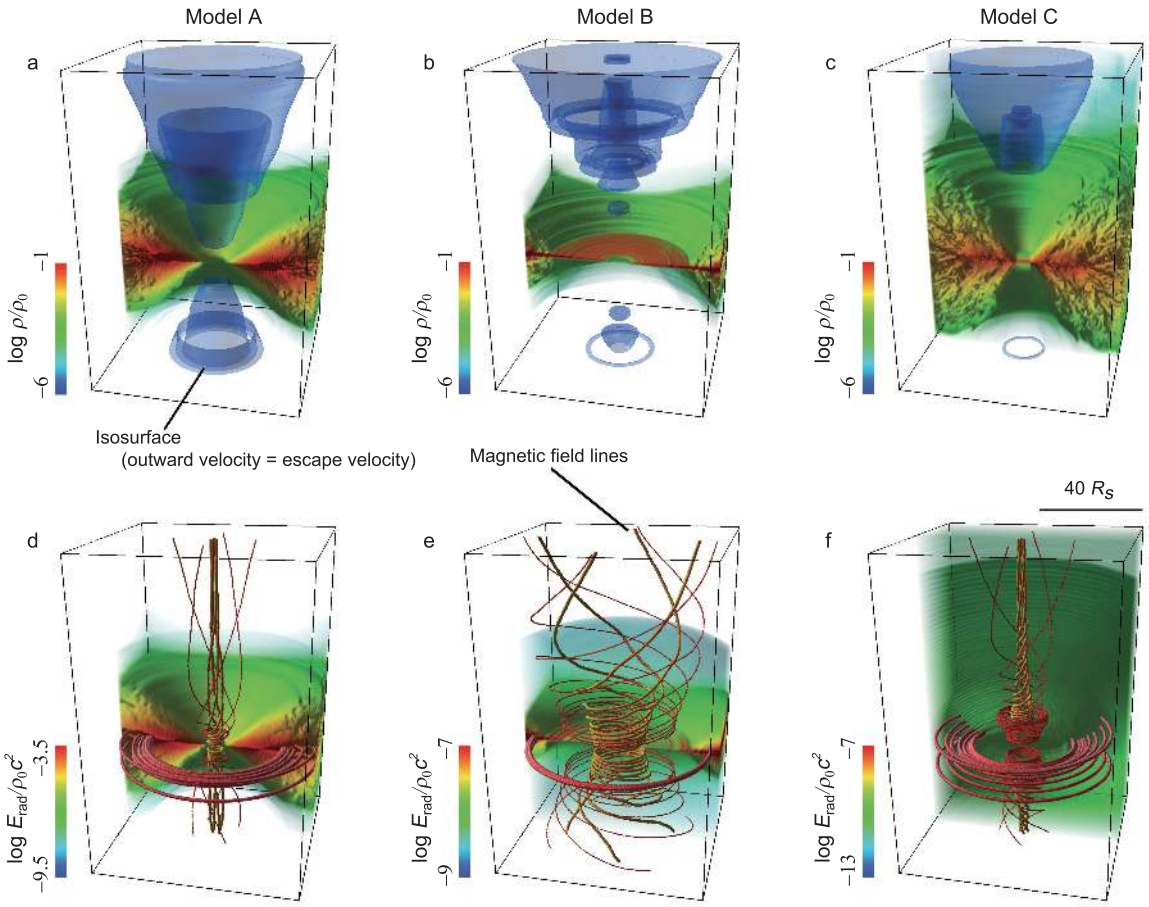

Fig. 1. Perspective view of inflow and outflow patterns near the black-hole for models A, B, and C, from left to right, respectively. Upper panels: Normalized density distributions (color) are overlaid with isosurfaces, at which the outward velocity equals to the escape velocity. Here, the elapse times are 5.25 s, 7.75 s, and 5.0 s for models A, B, and C, respectively. Lower panels: The distributions of the normalized radiation energy density (color) is overlaid with the magnetic-field lines. In models A and B, the green surfaces of the disks correspond to the photosphere, where the optical thickness measured from the upper ($z = 91.6\,R_S$) or lower ($z = -91.6\,R_S$) boundaries is unity. Note that the disk in model C is optically thin.

Table 1. Three calculated models and basic properties.

Model Corresponding States		A Slim disk	B Standard disk	C RIAF
Normalized mass accretion rate*	$\dot{M}_{\rm acc}/(L_{\rm E}/c^2)$	120	5.3×10^{-3}	5.8×10^{-5}
Eddington ratio*	$L/L_{\rm E}$	1.0	7.3×10^{-4}	7.4×10^{-10}
Ratio of outflow rate to accretion rate*	$\dot{M}_{\rm out}/\dot{M}_{\rm acc}$	0.045	0.013	0.1
Ratio of kinetic luminosity to luminosity*	$L_{\rm kin}/L$	0.16	0.0013	120
Density†	$\log \rho\,[{\rm g\,cm^{-3}}]$	$-1 \sim -2$	~ -5	~ -10
Gas temperature†	$\log T$ [K]	~ 8	~ 6	$10 \sim 11$
Gas energy density‡	$\log E_{\rm gas}$ [erg cm^{-3}]	15.0	9.7	9.0
Magnetic energy density‡	$\log E_{\rm mag}$ [erg cm^{-3}]	15.3	9.2	8.3
Radiation energy density‡	$\log E_{\rm rad}$ [erg cm^{-3}]	17.2	10.4	3.2
Plasma-β‡	$p_{\rm gas}/p_{\rm mag}$	0.33	2.1	3.3

* The mass accretion rate ($\dot{M}_{\rm acc}$) is evaluated the mass passing through the inner boundary near the black-hole ($r = 3\,R_S$ and $z < 3\,R_S$) per unit time, and outflow rates ($\dot{M}_{\rm out}$) indicate the mass passing through the upper boundary ($z = 91.6\,R_S$) with higher velocities than the escape velocity (high-velocity outflow) per unit time. The luminosity (L) is calculated based on the radiative flux at the upper boundary, and the kinetic luminosity ($L_{\rm kin}$) is calculated from the amount of the kinetic energy carried by the high-velocity outflow. These values are time-averaged over $t = 5.5$–6.0 s (models A and C) or $t = 7.5$–8.0 s (model B).

† Time-averaged over $t = 5.0$–6.0 s (models A and C) or $t = 7.0$–8.0 s (model B) at the regions $r = 10$–$20\,R_S$ and $z \sim 0$.

‡ Density-weighted spatial averages within the regions of $r = 10$–$20\,R_S$ and $z = 0$–$10\,R_S$ and are time-averaged over $t = 5.0$–6.0 s (models A and C) or $t = 7.0$–8.0 s (model B). Here, $p_{\rm gas}$ and $p_{\rm mag}$ are gas and magnetic pressures.

3.2. *Outflows*

As shown in figure 1, the disk outflows with helical magnetic fields are ubiquitous around black-holes. In models A and C the magnetic-field lines stretch out vertically in the vicinity of the rotation axis. While, around the equatorial plane, the toroidal component of the magnetic fields is dominant over other components in all models, which are reminiscent of magnetic-tower jets (Lynden-Bell 1996; Kato et al. 2004).

In model A, the strong radiation-pressure force is responsible for driving quasi-steady outflows above and below the disk, whose velocity amounts to $\sim 0.25c$. We have found that the radiation energy density ($E_{\rm rad}$) is very large in the disk region, and a steep profile of $E_{\rm rad}$ enhances the radiation force (radiative flux) (Ohsuga et al. 2005).

Remarkably, our simulation of model B shows the occurrence of a magnetically powered disk wind, contrary to the usual belief regarding the standard disk model. Note, however, that the disk wind is not very strong in model B; $L_{\rm kin} \ll L$ and $L_{\rm kin}/L$ is the smallest among all models, where $L_{\rm kin}$ is the kinetic luminosity. It must be stressed that we have solved the entire inflow-outflow structure simultaneously, unlike in previous simulations, in which the inflow (disk) structure was not solved, but treated as a boundary condition (Proga & Kallman 2004).

Our RMHD simulations reveal $L_{\rm kin}/L > 1$ in model C, in contrast with models A and B, implying that the disks with $\dot{M}_{\rm acc} \ll L_{\rm E}/c^2$ lose energy via jets rather than via radiation. The outflow rate is 10% of the mass-accretion rate, and the ratio is largest in three models. The photons freely escape from the disk, producing a quasi-spherical distribution of $E_{\rm rad}$, whereas the radiation energy is enhanced inside the disk in models A and B. The radiation force is negligible because of a small radiative flux.

The FLD approximation is good for models A and C, since the whole region (except for the very vicinity of the inner boundary) is optically thick for Thomson scattering in the former, and radiative cooling is never important in the latter. This is known to be problematic when determining the direction of the radiation flux in regions where the optical depth is around unity (e.g., around the disk surface in model B). We, however, wish to stress that the outflow is accelerated by magnetic pressure, and not by radiation force.

3.3. *Amplification of Magnetic Fields and Viscosity*

We have found that the magnetic energy ($E_{\rm mag}$) is amplified to be 30% and 20% of the gas energy ($E_{\rm gas}$) in models B and C, respectively (see table 1). In model A, surprisingly, $E_{\rm mag}$ does exceed the gas energy, $E_{\rm mag} \sim 2\,E_{\rm gas}$. Its implication is enormous: the viscosity had better be scaled in terms of the total (or radiation) pressure, and not of the gas pressure in radiation pressure-supported disks (cf. Sakimoto & Coroniti 1981).

This is one of the most significant issues in astrophysics: how to prescribe the disk viscosity. In figure 2 we show how the magnetic torque, $\langle -B_r B_\varphi/4\pi\rangle$, behaves as a function of the pressure in the region close to a black-hole (at $r = 5\,R_S$). We can see that the torque is roughly proportional to the total pressure (with some scatters) in all the cases. If we define the viscosity parameter as $\alpha = \langle -B_r B_\varphi/4\pi\rangle/\langle p_{\rm tot}\rangle$, where total pressure ($p_{\rm tot}$) is the sum of the gas pressure and the radiation energy density divided by 3, we estimate $\alpha \sim 0.004$, 0.006, and 0.002 for models A, B, and C, respectively.

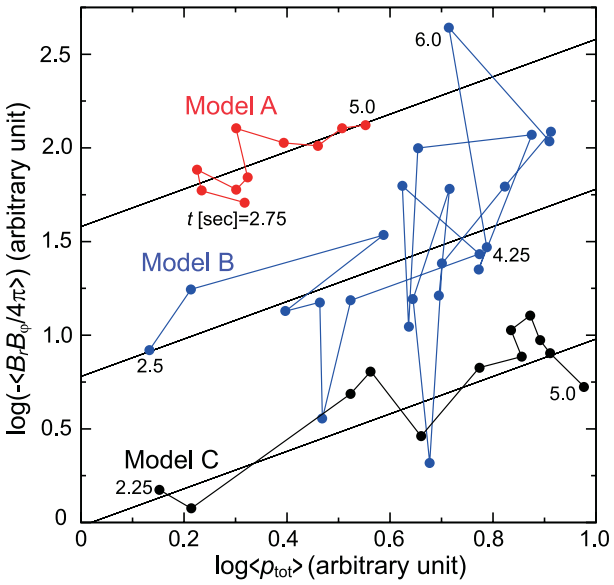

Fig. 2. The density-weighted spatial averages of the magnetic torque near the black-hole, $r = 5\,R_S$, as functions of the total pressure. Each point represents the time-averaged value for every 0.25 s. At the initial points, $(\log\left[-\langle B_r B_\varphi/4\pi\rangle\right], \log\langle p_{\rm tot}\rangle) \sim (15.3, 12.7)$, (10.9, 8.7), and (8.6, 5.8) in CGS unit for models A, B, and C, respectively.

Cautions should be taken concerning the point that the properties of magnetic fields in two-dimensional simulations could be affected by any artificial occurrence of channel modes of flow and the anti-dynamo theorem, and thus deviate from those of three-dimensional simulations. Hence, a three-dimensional study should be explored in future work.

4. Observational Implications

Outflows and jets are ubiquitous in any regimes of black-hole disk accretion flow. They seem to manifest themselves by warm absorption features of active galactic nuclei, and by blue-shifted absorption lines in black-hole binaries (BHBs) (Blustin et al. 2005; Cappi 2006; Kubota et al. 2007). High-velocity outflows with a velocity of $\sim 0.25c$ in model A will explain the X-ray observations of bright quasars exhibiting blue-shifted absorption lines, which are interpreted as being absorption by the outflow material moving with velocity on the order of $0.1c$ (Pounds et al. 2003; Reeves et al. 2003). Although no strong outflows were expected within the framework of the standard disk model, Miller et al. (2006) concluded by X-ray observations of BHB, GRO J1655−40, that the X-ray absorbing wind is ejected from the geometrically thin disk viewed at an inclination angle of $\sim 70°$. The density and the velocity of the wind were reported to be $\sim 10^{-9}\,{\rm g\,cm^{-3}}$ and $0.001c$–$0.05c$. Such features are roughly consistent with our simulation (model B), in which gas with $\rho =$ several $\times\ 10^{-10}\,{\rm g\,cm^{-3}}$ is blown away towards the diagonal direction (polar angle of $\sim 45°$) at a speed of $\sim 0.01c$. Our simulations show that the magnetic field lines

are along the jet axis (models A and C). Such a structure has been revealed by recent radio observations of polarized emission in a BL Lac object, Markarian 501 (Giroletti et al. 2008). A detailed comparison with observations is left as future work.

To summarize, our global RMHD simulations open a new era of accretion-disk research and provide a unified view of accretion flows in various contexts.

The computations were performed on a parallel computer at Rikkyo University, XT4 system at CfCA of NAOJ, Super Combined Cluster System at RIKEN, and computational facilities including the T2K Tsukuba and FIRST cluster at CCS in University of Tsukuba. This work is supported in part by Ministry of Education, Culture, Sports, Science, and Technology (MEXT) Young Scientist (B) 20740115 (KO), by the special postdoctoral researchers program of RIKEN (KO), by a Grant-in-Aid of MEXT (19340044, SM), by a Grant-in-Aid for the global COE programs on "The Next Generation of Physics, Spun from Diversity and Emergence" from MEXT (SM) and by a Grant-in-Aid of JSPS (14740132, MM).

References

Abramowicz, M. A., Czerny, B., Lasota, J. P., & Szuszkiewicz, E. 1988, ApJ, 332, 646
Balbus, S. A., & Hawley, J. F. 1991, ApJ, 376, 214
Blustin, A. J., Page, M. J., Fuerst, S. V., Branduardi-Raymont, G., & Ashton, C. E. 2005, A&A, 431, 111
Cappi, M. 2006, Astron. Nachr., 327, 1012
De Villiers, J.-P., Hawley, J. F., & Krolik, J. H. 2003, ApJ, 599, 1238
Eggum, G. E., Coroniti, F. V., & Katz, J. I. 1988, ApJ, 330, 142
Fragile, P. C., & Meier, D. L. 2009, ApJ, 693, 771
Giroletti, M., Giovannini, G., Cotton, W. D., Taylor, G. B., Pérez-Torres, M. A., Chiaberge, M., & Edwars, P. G. 2008, A&A, 488, 905
Hawley, J. F., & Krolik, J. H. 2001, ApJ, 548, 348
Hawley, J. F., & Krolik, J. H. 2006, ApJ, 641, 103
Hayashi, C., Hōshi, R., & Sugimoto, D. 1962, Prog. Theor. Phys., Suppl., 22, 1
Hirose, S., Krolik, J. H., & Stone, J. M. 2006, ApJ, 640, 901
Ichimaru, S. 1977, ApJ, 214, 840
Kato, S., Fukue, J., & Mineshige, S. 2008, Black-Hole Accretion Disks–Towards a New Paradigm (Kyoto: Kyoto University Press)
Kato, Y., Mineshige, S., & Shibata, K. 2004, ApJ, 605, 307
Koide, S., Shibata, K., Kudoh, T., & Meier, D. L. 2001, J. Korean Astron. Soc., 34, S215
Kubota, A., et al. 2007, PASJ, 59, S185
Levermore, C. D., & Pomraning, G. C. 1981, ApJ, 248, 321
Lynden-Bell, D. 1996, MNRAS, 279, 389
Machida, M., Hayashi, M. R., & Matsumoto, R. 2000, ApJ, 532, L67
Matsumoto, R. 1999, in Numerical Astrophysics, ed. S. M. Miyama, K. Tomisaka, & T. Hanawa (Dordrecht: Kluwer) 195
Miller, J. M., et al. 2006, Nature, 441, 953
Narayan, R., & Yi, I. 1994, ApJ, 428, L13
Ohsuga, K. 2006, ApJ, 640, 923
Ohsuga, K., Mori, M., Nakamoto, T., & Mineshige, S. 2005, ApJ, 628, 368
Okuda, T., & Fujita, M. 2000, PASJ, 52, L5
Paczynsky, B., & Wiita, P. J. 1980, A&A, 88, 23
Pounds, K. A., Reeves, J. N., King, A. R., Page, K. L., O'Brien, P. T., & Turner, M. J. L. 2003, MNRAS, 345, 705
Proga, D., & Kallman, T. R. 2004, ApJ, 616, 688
Rees, M. J., Begelman, M. C., Blandford, R. D., & Phinney, E. S. 1982, Nature, 295, 17
Reeves, J. N., O'Brien, P. T., & Ward, M. J. 2003, ApJ, 593, L65
Rubin, E. L., & Burstein, S. Z. 1967, J. Comput. Phys., 2, 178
Rybicki, G. B., & Lightman, A. P. 1979, Radiative Processes in Astrophysics (New York: John Wiley & Sons)
Sakimoto, P. J., & Coroniti, F. V. 1981, ApJ, 247, 19
Shakura, N. I., & Sunyaev, R. A. 1973, A&A, 24, 337
Turner, N. J., & Stone, J. M. 2001, ApJS, 135, 95
Turner, N. J., Stone, J. M., Krolik, J. H., & Sano, T. 2003, ApJ, 593, 992
Yokoyama, T., & Shibata, K. 1994, ApJ, 436, L197